P6.8

LONG-TERM VARIABILITY OF CONVECTIVE CLOUD VISIBLE ALBEDO FROM ISCCP COMPARED TO VIRS/MODIS

J. Colleen Mikovitz[1*], P. W. Stackhouse, Jr.[2], Y. Hu[2], B. A. Wielicki[2], S. J. Cox[1], and S. K. Gupta[1]

[1]Analytical Services and Materials, Inc., Hampton, VA
[2]NASA Langley Research Center, Hampton, VA

1. INTRODUCTION

While monitoring satellite visible calibration over long-time periods from satellite to satellite remains a difficult issue, it is critical to the derivation of long-term cloud and radiation data sets. Most of the work in this area focuses upon using earth targets in clear-skies (for a summary see Brest *et al* 1997). Spectral dependencies of various satellite instruments and surface properties along with atmospheric constituents such as aerosols affect these calibrations.

Here, we apply a methodology that uses the coldest-brightest pixels from deep tropical convective clouds. These clouds are relatively homogeneous and optically thick. The height of the clouds is such that spectrally dependent atmospheric scattering processes are minimized. The frequency of occurrence and microphysical properties of these clouds may change in time without significantly affecting the cloud reflectivity characteristics. This technique was first developed to verify Clouds and the Earth's Radiant Energy System (CERES) broadband SW channel calibration (Hu *et al* 2000). This method is adapted to evaluate its usefulness for AVHRR and geosynchronous visible channel observations from the International Satellite Cloud Climatology Project (ISCCP) inter-calibrated data set (Rossow and Schiffer, 2000). Seasonal processing is compared to the Visible Infrared Scanner (VIRS) visible channel and the CERES SW channel. The outline of the procedure follows:

•Use a brightness temperature threshold to find the coldest pixels in tropical convective areas.

•Compute visible reflectances and bin in terms of solar zenith, view zenith and relative azimuth angles.

•Apply anisotropic models to bin averaged reflectances to compute albedos.

* *Corresponding author address:* Colleen Mikovitz, AS&M, Suite 300, One Enterprise Parkway, Hampton, VA 23666-5845; email: J.C.Mikovitz@larc.nasa.gov

2. ISCCP PIXEL SELECTION AND REFLECTANCES

2.1 Pixel Screening

ISCCP DX pixels between 40°S and 40°N with window brightness temperatures less than 205K are chosen. This allows the deep convective clouds to be captured and ensures ample pixel sampling for statistical evaluation. The criteria are applied to the daytime ISCCP DX brightness temperatures from December 1984 through November 1995

2.2 Reflectance Calculations

ISCCP DX visible calibration gives a scaled radiance for each geosynchronous and sun synchronous instrument which are normalized relative to the AVHRR visible channel. This scaled radiance is given by:

$I_{isccp} = I_{cal} / S_o$

Where S_o is the solar constant at the mean earth-sun distance. The reflectance (r) is computed using:

$r = \pi^* I_{isccp} / \mu_o$

A correction for the earth-sun distance for the time of year is also included. These reflectances are subsequently binned using solar zenith, viewing zenith and relative azimuth angle bins of 5, 5, and 10 degrees, respectively. Additional pixel screening is done by eliminating pixels with values greater than 3 standard deviations from the bin average.

3. ANGULAR AVERAGED ALBEDOS

3.1. Narrowband Anisotropy from VIRS and Theory

Anisotropic factor is defined as:

$R = \pi^* I/F$

Where I is radiance and F is flux.

The anisotropy is derived from 9 months of VIRS observations for clouds with temperatures lower than 205K. Theoretical model results are adopted for missing bins. Model attributes:

•Single scattering properties: Improved geometric optics method (Yang and Liou, 1998)

•Particle shapes: a combination of different shapes (plates, columns and aggregates)

•Particle sizes and shapes are chosen by least square fitting to the available bins

•Radiative transfer: DISORT

•Molecular Absorptions: Correlated-K distribution (Kratz, personal communication)

Examples of the anisotropic functions for solar zenith angles 40° and 60° are shown in Figure 1.

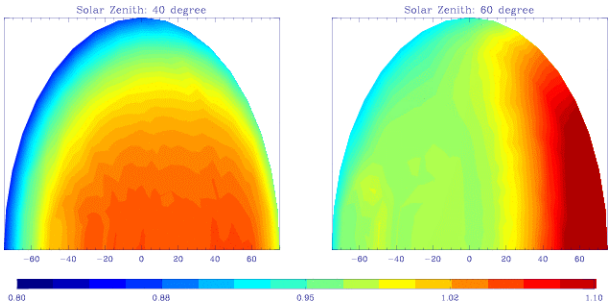

Figure 1. Anisotropic Functions for 40° and 60° solar zenith angles.

3.2 Derivation of Albedos

As a first approach, the albedos for each bin are computed using the anisotropy models from the VIRS/theory. Deriving albedo from reflectance gives:

$\alpha = r / R$

Figure 2 presents the results of using this approach to compute distribution functions of CERES albedos derived similarly for 9 months of data for all pixels with solar zenith angles (SZA) less than 60°. Note that the peak of the distribution is sharp and very stable for the 9 months, remaining within 0.01 of the peak value.

This approach is applied to the radiance and brightness temperatures from the ISCCP DX dataset for each of the polar orbiters and geosynchronous satellites included in that dataset. Figure 3 shows the distribution functions of each ISCCP satellite group for each year of March, April and May (MAM) for SZA less than 60°. The peak of these distributions does not show the same stability year to year as the CERES albedos. The best case in stability occurs with AVHRR instruments, where there is a 7.5% albedo difference between albedo bin peaks. GOES shows at least a 15% albedo difference between years. Changes in individual satellites for each group cannot totally account for the variability. In Fig. 3-b, some of the largest changes in peak distribution and distribution shape occur during the years 1990 and 1994 with GMS-4.

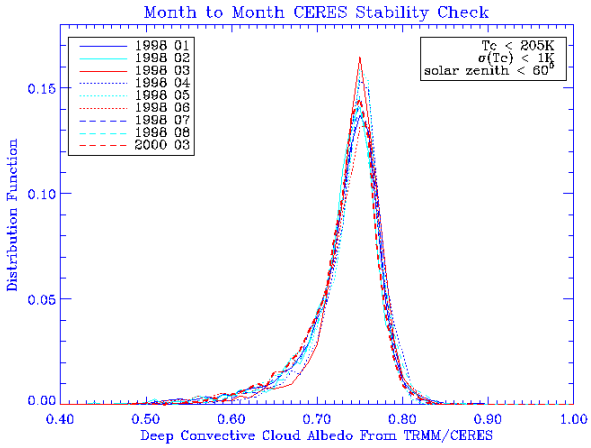

Figure 2. The distribution function of CERES albedos for 9 months for solar zenith angles <60°.

A summary of all of the seasons for each satellite group is given in Table 1. For each individual season, a mean, standard deviation, and peak distribution bin of albedo are calculated. Then seasonal averages of these components are calculated for each satellite, along with max and min peak distribution bins. VIRS seasons of MAM and JJA 1998 are included for comparison. For over half of these cases, the average albedo is one bin away from the average peak bin (e.g., DJF GOES bin peak is 0.862, while the average 0.844 would be in the bin 0.837). From both Fig. 3-c and Table 1, the distribution for GOES is skewed towards higher albedos. This average and peak matches more closely with the VIRS single season, but may be fortuitous because of the range of all GOES distributions. There is not a well-defined peak such as AVHRR (Fig.3-a) exhibits. Since MAM 1994 for each satellite in Fig. 3 has an odd distribution, a test excluding 1994 and 1995 data reduces the average standard deviation by up to 0.011 (MAM AVHRR).

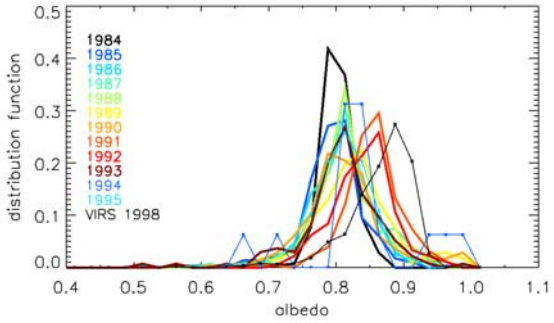

Figure 3-a. The distribution function of albedos for SZA < 60^o for AVHRR instruments for MAM season. This also includes 1998 MAM VIRS.

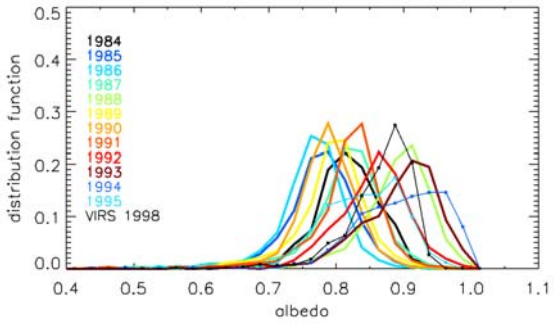

Figure 3-b. GMS

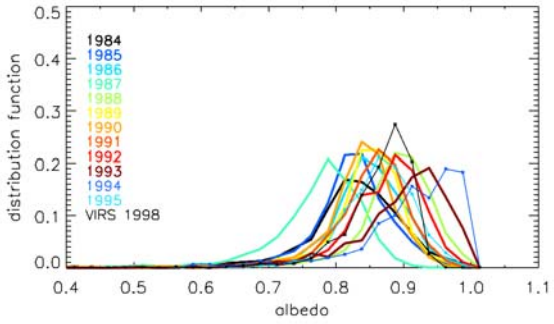

Figure 3-c. GOES

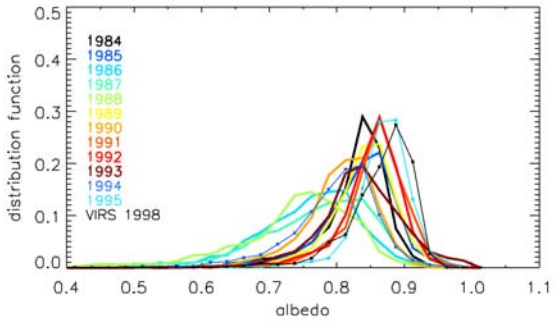

Figure 3-d. METEOSAT

Season	Sat.	Ave Alb	Max Bin Peak	Min Bin Peak	Ave Bin Peak	Ave Std. Dev.
DJF	AVHRR	0.811	0.838	0.788	0.813	0.0536
	MET	0.819	0.913	0.763	0.838	0.0656
	GMS	0.817	0.913	0.788	0.838	0.0602
	GOES	0.844	0.913	0.787	0.863	0.0801
MAM	AVHRR	0.822	0.863	0.788	0.813	0.0619
	MET	0.811	0.888	0.763	0.838	0.0649
	GMS	0.826	0.938	0.763	0.838	0.0579
	GOES	0.857	0.963	0.788	0.863	0.0645
(1998)	VIRS	0.863			0.888	0.0492
JJA	AVHRR	0.822	0.838	0.788	0.813	0.0476
	MET	0.829	0.888	0.813	0.863	0.0696
	GMS	0.838	0.938	0.763	0.838	0.0555
	GOES	0.861	0.988	0.813	0.863	0.0649
(1998)	VIRS	0.866			0.888	0.0409
SON	AVHRR	0.828	0.938	0.788	0.813	0.0524
	MET	0.841	0.913	0.763	0.838	0.0719
	GMS	0.842	0.938	0.788	0.838	0.0555
	GOES	0.860	0.913	0.788	0.863	0.0653

Table 1. Statistics for histogram distribution function of all seasons.

Another way to look at the calibration is to view the satellite groups as they relate to each other. Figure 4-a is the seasonally averaged albedo time series. Figure 4-b is the time series of the percentage difference each season's albedo is from the satellite's overall albedo average. This figure also limits the SZA less than 60^o. The albedo averages for these results are weighted by

the cosine of the SZA. Before mid-1994, the percent difference for AVHRR remains within 5%. The other three satellite groups show the same inconsistency as before with differences at times being greater than 15%, even excluding 1994 and 1995.

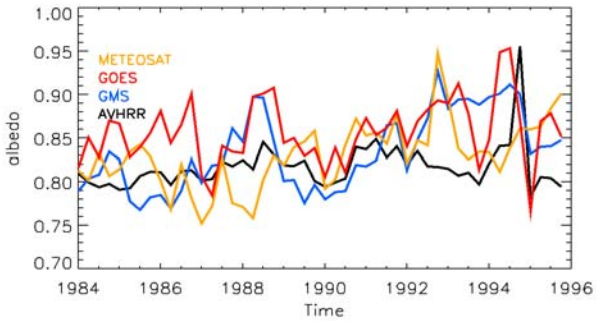

Figure 4-a. Seasonal albedo average time series for SZA<60°.

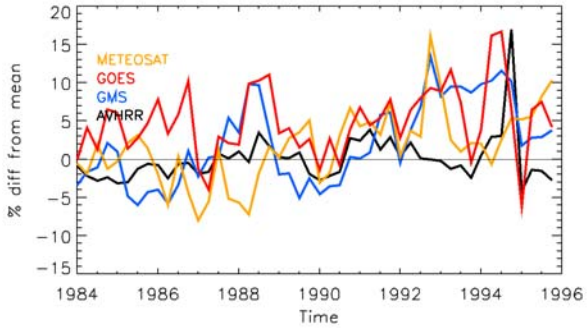

Figure 4-b. Albedo difference from average for SZA<60°

4. CONCLUSIONS

Using high cold bright pixels from mainly tropical convection, the ISCCP calibration is compared to VIRS and to CERES. The results show that the ISCCP calibration contains a large amount of variability from season to season and year to year. Analysis is required to explain the anomalies in the time series as shown in Figure 4-b. For instance, in late 1994 the AVHRR shows an anomaly that is 15% from average. This corresponds to a time when NOAA 11 equator overpass time was past 4 pm.

More work is required to better develop this method and to verify the angular models and spectral responses. This will ensure that the differences are less due to changing view angles and more due to calibration variability. Thus, the stability of the ISCCP calibration in time might be verifiable using this method. A better accounting for the spectral differences between VIRS and AVHRR and the geosynchronous instruments would provide an opportunity to inter-compare the albedos directly. ISSCP data sets already overlap the VIRS/CERES/MODIS observations and will be processed in the future to provide a more direct opportunity to relate ISCCP calibration methods to these observations. This is a crucial step in building long-term cloud and radiation data sets

Acknowledgements

We wish to thank Dr. Patrick Minnis of NASA Langley for providing the calibrated VIRS data and Dr. David Kratz also of NASA Langley for providing correlated-k data over the instrument spectral response functions. This work was funded by NASA grant MDAR-0506-0383 under the EOS Interdisciplinary Science program (NRA-99-OES-04)

References

Brest, C.L., W.B. Rossow, M.D. Roiter, 1997: Update of radiance calibrations for ISCCP. *J. Atmos. Ocean. Tech.* **14,**1091-1109.

Hu, Y and B. Wielicki, 1999: Deep convective cloud albedo studies from TRMM CERES, VIRS and PR. Proceedings of 10th AMS Atmospheric Radiaiton Conferences.

Rossow, W.B. and R.A. Schiffer, 2000: Advances in understanding clouds from ISCCP. *Bull. Amer. Soc.,* **80,** 2261-2287.

Yang, P. and K.N. Liou, 1998: Single-scattering properties of complex crystals in terrestrial atmosphere. *Contr. Atmos. Phys.*, **71**, 223-248.